g factors of the 9^- and 11^- isomers in ^{194}Pb and ^{196}Pb: Configuration mixing and deformation

K. Vyvey,[1,2] G. D. Dracoulis,[1] A. N. Wilson,[1] P. M. Davidson,[1] A. E. Stuchbery,[1]
G. J. Lane,[1] A. P. Byrne,[1,3] and T. Kibédi[1]
[1]*Department of Nuclear Physics, Australian National University, Canberra, ACT 0200, Australia*
[2]*Instituut voor Kern- en Stralingsfysica, University of Leuven, Celestinjnenlaan 200 D, B-3001 Leuven, Belgium*
[3]*Department of Physics, The Faculties, Australian National University, Canberra, ACT 0200, Australia*
(Received 11 February 2004; published 17 June 2004)

The g factors of the 9^- and 11^- yrast states in ^{194}Pb and ^{196}Pb have been measured using the time-dependent perturbed angular distribution (TDPAD) technique. An analysis of the systematics of the properties of these states in the light Pb isotopes is presented. The results confirm the dominance of the $\nu(2f_{5/2}^{-1}1i_{13/2}^{-1})$ configuration in the 9^- isomer. The values for the 11^- isomers are consistent with the $\pi(3s_{1/2}^{-2}1h_{9/2}1i_{13/2})$ configuration, but they are smaller than those in the Po isotones. The effects of core excitation and particle-vibration coupling are considered, but these do not lead to a detailed agreement between theory and experiment. A Nilsson approach, however, gives good agreement, providing support for a proposed oblate deformation.

DOI: 10.1103/PhysRevC.69.064318 PACS number(s): 21.10.Ky, 21.60.−n, 27.80.+w

I. INTRODUCTION

The structure of the low-lying isomeric states in the Pb isotopes near the closed neutron shell at $N=126$ is, in general, well understood, with predominantly spherical configurations assigned and confirmed by spectroscopic studies, including g-factor measurements [1,2]. In moving away from the $N=126$ closed neutron shell, however, only the $\nu(1i_{13/2}^{-2})_{12^+}$ states in the even Pb isotopes have been extensively investigated by g-factor measurements. The systematic fall of these g factors as a function of reducing the neutron number has been interpreted as a consequence of the emptying of the $\nu(1i_{13/2})$ orbital, resulting in reduced $(1i_{13/2}\rightarrow 1i_{11/2})$ core polarization effects [3,4].

In this work we present experimental results on the g factors of the 9^- and the 11^- yrast states in ^{194}Pb and ^{196}Pb. The new measurements, combined with published results [5–11], allow the change in the main components of the 9^- wave functions to be traced as a function of the neutron number. While the 9^- isomers are constructed from valence neutron-hole configurations which, in general, have small negative g factors, the 11^- isomers are proton excitations out of the $Z=82$ core, so that their g factors are usually large and positive. Because of the difference in valence configuration and the different sensitivity to core excitation, their g factors will be influenced by different factors. For example, particle-quadrupole vibration coupling is likely to become more important as the neutron shell is depleted. In the case of the 11^- isomers in particular, particle-octupole vibration coupling admixtures could also affect the g factors. Furthermore, the 11^- isomers in the neutron-deficient isotopes are predicted to be deformed, an effect which is partly related to the core excitation involved in their formation. In the final analysis, vibrational coupling is shown not to be significant for the Pb cases, whereas the moderate oblate deformation predicted for the 11^- isomers is.

The 11^- states in ^{196}Pb [7] and ^{198}Pb [8] are the only ones measured, to date, in the Pb region that allow for a direct comparison of the g factor of a $2p$-$2h$ state and its corresponding $2p$ state with the same neutron number. The values, $g(^{194}\mathrm{Pb};11^-)=0.96(8)$ and $g(^{198}\mathrm{Po};11^-)=1.10(5)$, differ more than expected from the particle-core coupling model [12], which predicts a value of about 1.09(2) for ^{196}Pb. If the deformation in the light Pb cases is indeed well defined, a Nilsson approach is justified, but while the previously measured g factor of the ^{194}Pb(11^-) isomer is in agreement with the Nilsson value, the experimental error is too large for the comparison to be decisive.

Therefore, to address such questions and to allow an analysis of a broader range of isotopes, we have remeasured the g factor of the 11^- isomer in ^{196}Pb and measured the g factor of the equivalent isomer in ^{194}Pb. New results for the 9^- isomers are obtained in the same measurements.

II. EXPERIMENTAL TECHNIQUES AND RESULTS

The g factors of the isomeric states in ^{196}Pb and ^{194}Pb were measured by applying the time-dependent perturbed angular distribution technique [13]. Excited states were populated in the $^{170}\mathrm{Er}(^{30}\mathrm{Si},4n)^{196}\mathrm{Pb}$ and the $^{170}\mathrm{Er}(^{29}\mathrm{Si},5n)^{194}\mathrm{Pb}$ reactions at beam energies of 136 and 143 MeV, respectively. The beams, delivered by the ANU 14 UD accelerator, were arranged to give $\sim$1 ns wide pulses with a separation of 960 ns for ^{196}Pb, and 1920 ns for ^{194}Pb, chosen after consideration of the requirements of sufficient yield and the longer lifetimes in the isomers of interest in ^{194}Pb. The states and transitions of interest are shown in the partial level scheme of Fig. 1 [14–16].

The target consisted of 0.7 mg/cm^2 metallic Er, enriched in ^{170}Er to 97%, on which a 6.6 mg/cm^2 Pb layer was evaporated to stop recoiling Pb nuclei. The projectiles came to rest in a thick Pb backing. The target was placed between the pole tips of an electromagnet, with an external magnetic field of 2.48(2) T applied perpendicular to the beam-detector plane. The magnetic field was measured with a Hall probe and calibrated internally using the precisely known g factors of the 12^+ isomers in ^{194}Pb and ^{196}Pb [3,6]. Gamma rays

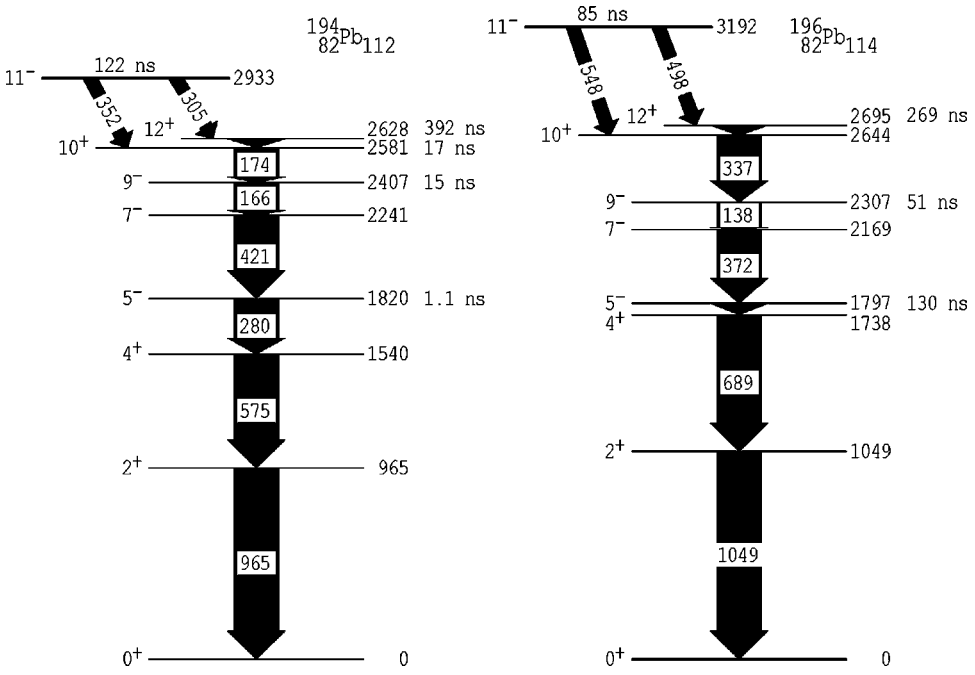

FIG. 1. The partial-level schemes. Half-lives from earlier measurements are shown for the isomeric states.

were observed in two Ge detectors of similar characteristics, positioned at ±135° with respect to the beam direction.

The data were analyzed by forming two-dimensional matrices of energy versus time, for each detector. From these matrices, time-gated energy spectra and energy-gated time spectra were constructed. Samples of the delayed γ-ray spectra for ^{196}Pb and ^{194}Pb are shown in Fig. 2, for the relevant energy regions.

In the initial analysis, the 498 keV, $\Delta I=1$ $E1$ transition from the 11^- isomer and the 372 keV $\Delta I=2$ $E2$ ($7^-\rightarrow 5^-$ transition) were used to extract the g factors of the 11^- and 9^- states in ^{196}Pb, respectively. For ^{194}Pb, the 352 and 305 keV $E1$ transitions were used to deduce the g factor of the 11^- isomer, whereas all $E2$ transitions below the 9^- state

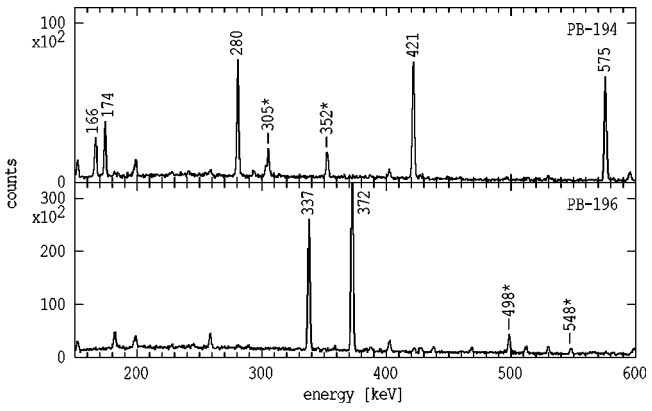

FIG. 2. Typical delayed spectra for a single detector obtained from the ^{170}Er(^{29}Si,5n) (upper panel) and the ^{170}Er(^{30}Si,4n) (lower panel) reactions. Transitions directly from the 11^- isomers are indicated with asterisks. The delayed time windows begin directly after the beam pulse and have widths of 550 and 450 ns, respectively. For clarity, a spectrum obtained with a gate on a later time period (when the isomers of interest have predominantly decayed) has been subtracted to remove activities.

were summed to extract a value for $g(^{194}\mathrm{Pb},9^-)$. The short lifetime (1.1 ns) and the small g factor of the 5^- (two-neutron-hole) state, which intervenes in the cascade, combine to have a negligible effect on this analysis.

The half-lives of 17(4) and 47(4) ns obtained for the 9^- states in ^{194}Pb and ^{196}Pb, and the values of 133(15) and 85(3) ns for the corresponding 11^- isomers, are in agreement with those obtained from former experiments [14,16]. From the time spectra $I(t,\theta,B)$, in which θ denotes the angle of the detectors with respect to the beam axis, the experimental modulation ratios $R(t,\theta,B)$ were formed in the standard way:

$$R(t,\theta,B)=\frac{I(t,\theta,B)-I(t,\theta+90^\circ,B)}{I(t,\theta,B)+I(t,\theta+90^\circ,B)}. \tag{1}$$

After a correction for the difference in detector efficiencies, the magnitude and sign of the nuclear g factors were extracted by using a least-squares fitting program based on the multilevel formulation given by Häusser *et al.* [11], a formulation which takes into account sequences of isomers. Samples of the ratio functions with fits are shown in Fig. 3. The g factors were deduced both from fits to the initial time spectra, and also to ratio functions such as these. The values obtained were

$$\begin{aligned} g(^{196}\mathrm{Pb},11^-) &= +1.04(5),\\ g(^{194}\mathrm{Pb},11^-) &= +1.03(2),\\ g(^{196}\mathrm{Pb},9^-) &= -0.037(10),\\ g(^{194}\mathrm{Pb},9^-) &= -0.042(15). \end{aligned} \tag{2}$$

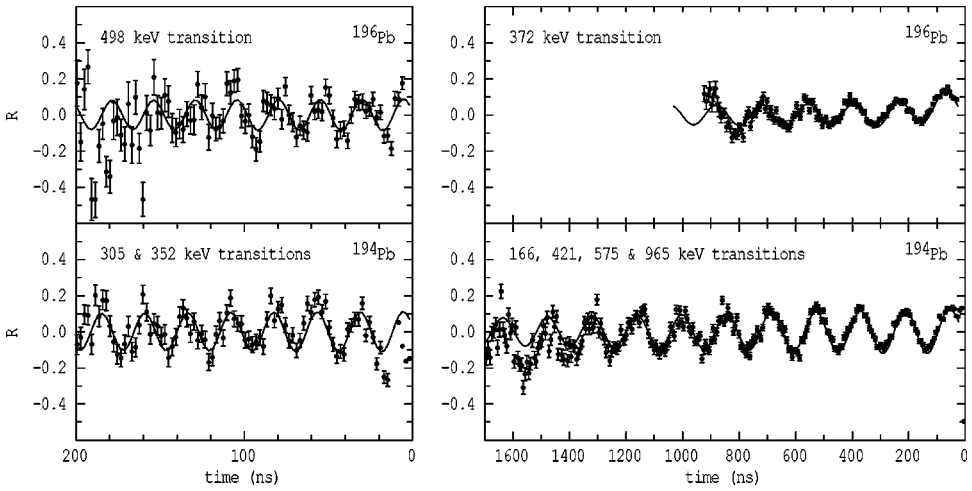

FIG. 3. The ratio functions with representative fits. (Note that these correspond to only part of the analysis.) On the left are shown the results for transitions from the 11^- isomers as indicated, while on the right, the fits from which the 9^-, g factors were deduced are shown. (Note also that the main oscillations in the latter spectra arise from the feeding from the 12^+ isomers.)

These values are corrected for Knight shift (K) and diamagnetic shielding (σ): $K(\text{Pb in Pb})=1.5(1)\%$ [17] and $\sigma(\text{Pb})=-1.0(1)\%$ [18]. Note that the values extracted for ^{194}Pb(9^-) and ^{196}Pb(11^-) are in agreement with the earlier values of $g(^{194}\text{Pb},9^-)=-0.07(4)$ (Ref. [6]) and $^{196}\text{Pb},11^-)=+0.96(8)$ (Ref. [7]), but they are more accurate.

III. DISCUSSION

A. Background

It is widely accepted that near $N=126$, the wave function of the 9^- yrast state consists mainly of the $\nu(2f_{5/2}^{-1}1i_{13/2}^{-1})$ neutron configuration [5,9,19]. This assumption is confirmed by g-factor measurements in ^{200}Pb and ^{202}Pb and several theoretical calculations [19–21]. The calculations of Pautrat *et al.* [21] predicted that in the neutron-deficient cases, the $\nu(2f_{7/2}^{-1}1i_{13/2}^{-1})$ excitation would be more significant, becoming the main configuration in ^{194}Pb. However, the more recent calculations of Pomar *et al.* [19] predict that although the $\nu(2f_{7/2}^{-1}1i_{13/2}^{-1})$ component will increase with decreasing neutron number, the $\nu(2f_{5/2}^{-1}1i_{13/2}^{-1})$ configuration will remain dominant. As g factors are particularly sensitive to core polarization effects that couple the spin-orbit partners ($f_{7/2}\rightarrow f_{5/2}$), the g-factor measurements allow some limits to be placed on the intensity of the $\nu(2f_{7/2}^{-1}1i_{13/2}^{-1})$ component in the wave function.

The structure of the 11^- isomers is totally different. Since their discovery, they have been associated with $2p$-$2h$ excitations across the $Z=82$ shell gap, involving a $\pi(3s_{1/2}^{-2}1h_{9/2}1i_{13/2})$ configuration. Experimental evidence originated from spectroscopic studies [14] and an early g-factor measurement [7]. Their low excitation energies ($\simeq$3 MeV compared to the 7 MeV predicted by the spherical shell model) have been attributed to enhanced pairing correlations and a move to oblate deformation, where the $s_{1/2}$ (below-shell) and $h_{9/2}$ (above-shell) proton orbitals are in close proximity, in contrast to the neutron excitations which are nearly spherical. Indeed, mean-field theoretical calculations result in predicted deformations ranging from $\beta_2=-0.15$ for the 11^- state in ^{198}Pb to $\beta_2=-0.19$ in ^{184}Pb [22,23].

More recent experiments [24] revealed surprisingly enhanced $E3$ strengths for the 11^- to 8^+ transitions in the even neutron-deficient Pb isotopes with $N\leqslant 114$. This phenomenon was also partly explained by invoking configuration mixing caused by the moderately deformed oblate shapes [24] and more direct evidence for a moderate deformation comes from measurement of the quadrupole moments of the 11^- isomers in ^{194}Pb and ^{196}Pb [25,26]. In a microscopic sense, the collectivity and deformation arise from the increase of the number of valence particles ($2p$-$2h$ in the intruder states of Pb, compared to $2p$ in the regular ones of Po), leading to enhanced proton-neutron interactions and induced core-polarization effects. Calculations within the framework of the particle-core model were able to account for the factor of 2 increase of the quadrupole moments in the Pb cases compared to those of the corresponding 11^- isomers in the Po isotones [27].

The question arises whether the $2p$-$2h$ character influences the magnetic moments. The particle-core model predicts small second-order effects only [28,29]. As indicated earlier, if an oblate deformation is well developed for the 11^- isomers, as seems to be implied through both the results of mean-field calculations and the quadrupole moment measurements, a Nilsson model approach should also be an appropriate alternative.

A further question that will be addressed below is whether the octupole-coupled admixtures that are necessary to explain the enhanced $E3$ transitions in the decay of the 11^- isomers [24] should be reflected in the g factors.

B. The g factors of the 9^- isomers

The systematics of the g factors of the 9^- states in the even Pb isotopes given in Fig. 4 show a clear decrease with decreasing neutron number. This change can be attributed to the increasing contribution of the $\nu 2f_{7/2}\rightarrow\nu 2f_{5/2}$ spin-flip transition and the decreasing contribution of the $\nu 1i_{11/2}\rightarrow\nu 1i_{13/2}$ spin-flip transition [3,4] when going away from the closed $N=126$ shell. The Pauli principle excludes the $\nu 2f_{7/2}\rightarrow\nu 2f_{5/2}$ transition at the closed neutron shell, but the emptying of the $\nu 2f_{5/2}$ orbit will increase the probability for such contributions. Conversely, excitations from the $\nu 1i_{13/2}$

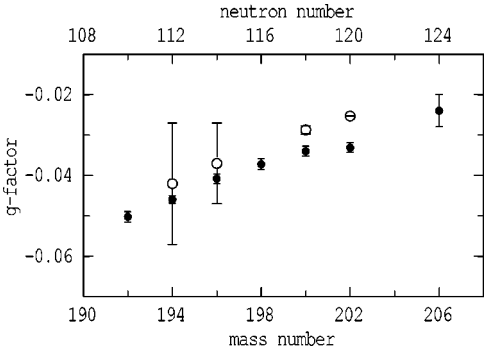

FIG. 4. A comparison between the experimental results (empty symbols) and theoretical calculations (filled symbols) for the g factors of the 9^- isomers in Pb.

orbit to the (empty) $1i_{11/2}$ orbit will be more probable when the $\nu 1i_{13/2}$ orbit is more occupied, i.e., when the neutron number is closer to $N=126$.

The g factor of a pure two-particle state $|j_1 j_2 J\rangle$ is calculated from the generalized Landé formula [30]

$$g_J = \frac{1}{2}(g_1+g_2) + \frac{1}{2}(g_1-g_2)\frac{j_1(j_1+1)-j_2(j_2+1)}{J(J+1)}. \quad (3)$$

The g factors of the $\nu 1i_{13/2}$ states are known experimentally from measurements on the $(\nu 1i_{13/2}^{-2})_{12^+}$ states in the range of isotopes, $^{192-206}$Pb [1,2] and the g factors of the $(2f_{5/2}^{-1})$ states have been measured in the odd isotopes, $^{201-207}$Pb. Hence, a straightforward approach is to combine the experimental values for the different mass numbers by means of Eq. (3) to give $g_{theo}(9^-)$. [Extrapolated/interpolated values need to be used for $g_{exp}(2f_{5/2}^{-1})$ for the lighter isotopes.] The values used and results are listed in Table I, and compared to the experimental values $g_{exp}(9^-)$ in Fig. 4. Note the deviation between experiment and theory for $A=200$ and $A=202$, where the experimental g factors are measured with the highest accuracy.

It is useful to put some limits on the intensity of any $\nu(2f_{7/2}^{-1}1i_{13/2}^{-1})_{9^-}$ component in the wave function of the 9^- state. If the experimental values are taken for $g(\nu 2f_{5/2}^{-1})$ in Eq. (3), however, the $\nu 2f_{7/2} \rightarrow \nu 2f_{5/2}$ contribution to the g factor is included implicitly. A better approach for extracting the amplitude of the $(\nu 2f_{7/2}^{-1}1i_{13/2}^{-1})_{9^-}$ contribution is, therefore, to combine the experimental g factors of the $\nu 1i_{13/2}^{-1}$ states in the different Pb isotopes, with the experimental g factor of the $\nu 2f_{5/2}^{-1}$ state in ^{207}Pb, in which the $f_{7/2}^{-1}$ contribution will be negligible. The main difference between $g(\nu 2f_{5/2}, ^{207}\mathrm{Pb})$ and $g(\nu 2f_{5/2}, ^{A<207}\mathrm{Pb})$ should be due to the increasing $\nu 2f_{7/2} \rightarrow \nu 2f_{5/2}$ contribution for the decreasing neutron number.

We assume for simplicity that the wave function contains only two components,

$$|9^-, ^A Pb\rangle = \alpha|2f_{5/2}^{-1}1i_{13/2}^{-1}\rangle + \sqrt{1-\alpha^2}|2f_{7/2}^{-1}1i_{13/2}^{-1}\rangle, \quad (4)$$

which is a reasonable assumption according to the calculations of Pomar *et al.* [19]. The main components of the g factor will be

$$g(9^-) = \alpha^2 g(2f_{5/2}^{-1}1i_{13/2}^{-1}) + 2\alpha\sqrt{1-\alpha^2}\Delta g + (1-\alpha^2)g(2f_{7/2}^{-1}1i_{13/2}^{-1}), \quad (5)$$

in which Δg arises from the off-diagonal matrix element between the spin-orbit pair $2f_{7/2}; j_1 = l + 1/2$ and $2f_{5/2}; j_1' = l - 1/2$. We can calculate Δg by following the detailed formalism given in Ref. [9], which is not repeated here. To calculate $g(2f_{7/2}^{-1}1i_{13/2}^{-1})$, we make use of the Schmidt value for $g(2f_{7/2})$. [Note that because of the small contribution of $g(2f_{7/2}^{-1}1i_{13/2}^{-1})$ to $g(9^-)$, the results obtained for the amplitude α are rather insensitive to the choice of $g(2f_{7/2})$.]

By combining $g(2f_{5/2}^{-1}1i_{13/2}^{-1})$, Δg, and $g(2f_{5/2}^{-1}1i_{13/2}^{-1})$ to obtain $g(9^-)$, and comparing the result to experiment, upper limits can be placed on the amplitudes of the $(2f_{7/2}^{-1}1i_{13/2}^{-1})$ components. The assumed values and results are listed in Table II. The amplitudes extracted are in rather good agreement with the calculations of Pomar *et al.* [19] and they exclude the dominance of the $(2f_{7/2}^{-1}1i_{13/2}^{-1})$ component for mass numbers $\leqslant 194$ predicted by Pautrat [21].

C. The g factors of the 11^- isomers

To gain some insight into both the neutron-number dependencies and the possible effects of breaking of the proton

TABLE I. Results for the calculated magnetic moments of the 9^- isomers in Pb.

A	$g_{exp}(12^+)$[a,b]	$A(2f_{5/2})$	$g_{exp}(2f_{5/2})$[a,b]	$g_{theo}(9^-)$	$g_{exp}(9^-)$
192	−0.173(2)	193	*+0.269(2)*	−0.0502(13)	⋯
194	−0.167(1)	195	*+0.269(2)*	−0.0459(9)	−0.042(15)[c]
196	−0.160(2)	197	*+0.269(2)*	−0.0408(12)	−0.037(10)[c]
198	−0.155(2)	199	*+0.269(2)*	−0.0372(13)	⋯
200	−0.151(2)	201	+0.2701(2)	−0.0340(12)	−0.0287(10)[a]
202	*−0.151(2)*	203	+0.2746(2)	−0.0331(12)	−0.02529(8)[a]
204	⋯	205	+0.02847(2)	⋯	⋯
206	−0.150(2)	207	+0.320(12)	−0.024(4)	

[a]Taken from Ref. [1].
[b]Estimated values are given in italics.
[c]This work.

TABLE II. Amplitudes of the $|2f_{5/2}^{-1}1i_{13/2}^{-1}\rangle$ and $|2f_{7/2}^{-1}1i_{13/2}^{-1}\rangle$ components in the wave functions of the 9^- isomers (see also the text).

A	$g_{exp}(12^+)$[a]	$g_{exp}(2f_{5/2})$[a,b]	$g_{exp}(9^-)$	α	$\sqrt{1-\alpha^2}$
194	−0.167(1)	+0.320(12)	−0.042(15)[c]	>0.990	<0.139
196	−0.160(2)	+0.320(12)	−0.037(10)[c]	>0.992	<0.122
198	−0.155(2)	+0.320(12)	⋯	⋯	⋯
200	−0.151(2)	+0.320(12)	−0.0287(10)[a]	>0.999	<0.049
202	*−0.151(2)*	+0.320(12)	−0.02529(8)[a]	>0.999	<0.052

[a]Taken from Ref. [1].
[b]Value for ^{207}Pb.
[c]This work.

core (as required in Pb but not in Po) all g factors measured to date for the 11^- isomers in the even Po and Pb isotopes are summarized in Fig. 5.

Although several of these are not known accurately, the g factor measured here for ^{194}Pb is significantly lower than the Po cases, most of which have values close to the spherical limit, exemplified by the value of $g=+1.109(8)$ for ^{210}Po [11]. Since quadrupole-vibrational admixtures were shown to be significant for reproducing the quadrupole moments of the 11^- isomers in ^{194}Pb and ^{196}Pb, we first examine the effect of these admixtures on the magnetic moment in the Pb cases, and for completeness, the Po cases as well.

1. Influence of the particle-quadrupole vibration coupling on the magnetic moments

For the Pb cases, a simple two-dimensional approach was taken previously to explain the quadrupole moments, by coupling the valence protons ($\pi 1i_{13/2}1h_{9/2}$) to the quadrupole vibrations of the underlying Hg core [27]. Perhaps surprisingly, it was found that the wave functions contained an important contribution from $|11^-\otimes 2_1^+;11^-\rangle$ admixtures. Because the magnetic moment operator is a tensor operator of order-1 (in contrast to the order-2 electric quadrupole operator), the influence of these admixtures on the magnetic moment is expected to be very small [28]. A comparison of the g factors of the $\pi 3s_{1/2}^{-2}1h_{9/2}$ intruder states in the Tl isotopes with the $\pi 1h_{9/2}$ (normal) states in the Bi isotopes revealed very little sensitivity to the second-order core polarization [12]. Nevertheless, in Ref. [29] it is claimed that the differences in quadrupole-vibrational admixtures of the form $2^+\otimes\pi d_{3/2}$ in the wave functions of the $\pi s_{1/2}$ states in ^{203}Tl, ^{205}Tl, and ^{207}Tl, caused by the differences in excitation energies of the states in the core nuclei, ^{204}Pb, ^{206}Pb, and ^{208}Pb, are sufficient to explain the significant neutron-number dependence of the Tl magnetic moments.

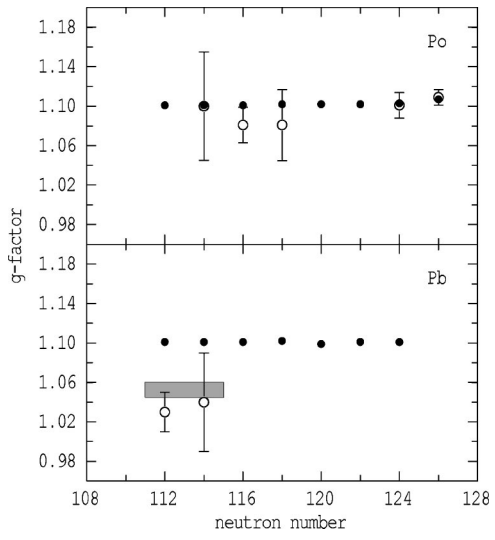

FIG. 5. A comparison between the experimental results (open symbols) and particle-quadrupole vibration calculations (filled symbols) for the 11^- isomers in Pb (lower panel) and Po (upper panel). The shaded area in the lower panel indicates the prediction for oblate deformation.

In the present case we have used the mixed wave functions, $|\widetilde{11^-}\rangle = a|11^-_{s.p.}\rangle + b|11^-_{s.p.}\otimes 2_1^+;11^-\rangle$, of Ref. [27] to calculate the magnetic moments of the 11^- isomers. Here, $|11^-_{s.p.}\rangle$ is a shorthand notation for $|1h_{9/2}1i_{13/2};11^-\rangle$, and $|2_1^+\rangle$ represents the first excited quadrupole vibrational state of the core. Note that the two-dimensional approach is semiempirical. Hence, the coefficients a and b can only be calculated if values for the $B(E2;0^+\rightarrow 2_1^+)$ transition probabilities, and the energies, $\hbar\omega_2$, of the $|2_1^+\rangle$ quadrupole vibrational states of the underlying cores are known. This is only the case for some of the Hg cores ($^{204-198}$Hg and ^{186,184}Hg [31]), hence interpolated values for $B(E2;0^+\rightarrow 2_1^+)$ are used where necessary, in order to calculate the complete Pb chain.

For comparison, the magnetic moments of the 11^- isomers in the Po chain have also been calculated using a Pb core. As experimental values for $B(E2;0^+\rightarrow 2_1^+)$ are only available for $^{204-208}$Pb, extrapolations have been made for the lighter isotopes such that the measured values for the spectroscopic quadrupole moments of the 8^+ isomers in Po, were reproduced by the two-dimensional calculations.

By using the wave functions as described above, the following expression for the magnetic moment is obtained:

$$\langle\widetilde{11^-}|\mu|\widetilde{11^-}\rangle = a^2\langle 11^-_{s.p.}|\mu|11^-_{s.p.}\rangle + b^2\langle 11^-_{s.p.}\otimes 2_1^+;11^-|\mu|11^-_{s.p.}\otimes 2_1^+;11^-\rangle. \quad (6)$$

The second-order term can be calculated by using the

TABLE III. The core parameters and results of the particle-quadrupole vibration calculations for the calculated g factors of the 11^- isomers in Pb.

isomer	A	N	A_{core} (Hg)	$B(E2;\text{core})^{a,c}$ $[e^2b^2]$	$g(2_1^+;\text{core})^{b,c}$	g^{2dim}	g^{exp}
Pb(11^-)	206	124	204	0.427	0.43(7)	1.101	⋯
	204	122	202	0.612	0.41(3)	1.101	⋯
	202	120	200	0.853	0.31(2)	1.099	⋯
	200	118	198	0.990	0.38(3)	1.102	⋯
	198	116	196	*1.10*	*0.4*	1.101	⋯
	196	114	194	*1.39*	*0.4*	1.101	1.04(5)
	194	112	192	*1.59*	*0.4*	1.101	1.03(2)

[a]Taken from Ref. [31].
[b]Weighted mean of values from Ref. [33].
[c]Values in italics estimated from extrapolations/interpolations.

Wigner-Eckart theorem and the reduction rules for tensor operators (see, e.g., Ref. [32]):

$$\begin{aligned}\langle 11^-_{s.p.}\otimes 2^+_1;11^-\|\mu\|11^-_{s.p.}\otimes 2^+_1;11^-\rangle &= -\begin{Bmatrix}11 & 2 & 11\\ 11 & 1 & 11\end{Bmatrix}23\langle 11^-_{s.p.}\|\mu\|11^-_{s.p.}\rangle \\ &\quad -\begin{Bmatrix}11 & 2 & 11\\ 1 & 11 & 2\end{Bmatrix}23\langle 2^+_1\|\mu\|2^+_1\rangle. \end{aligned} \quad (7)$$

The magnetic moment of the $|2_1^+\rangle$ state is estimated as $\mu_{obs}(2_1^+)=0.028\mu_N$ and $\mu_{obs}(2_1^+)=0.012\mu_N$ for the heavier and lighter Pb cores, respectively (see Table I) [33]. For the $^{204\text{-}198}$Hg cores, we use the experimental values of Ref. [33], while for the lighter Hg cores, we adopt the extrapolated value of $\mu_{obs}(2_1^+)=1.0\mu_N$. We take the magnetic moment of the 11^- state in ^{210}Po, $\mu=+12.20(9)$ [11], to approximate $\mu(11^-_{s.p.})$. By applying the Wigner-Eckart theorem again we can calculate the values for $\langle 11^-_{s.p.}\otimes 2^+_1;11^-|\mu|11^-_{s.p.}\otimes 2^+_1;11^-\rangle$ and obtain $\mu(\widetilde{11^-})$ and, therefore, the g factors as listed for the Pb cases in Table III.

Figure 5 compares the results of the calculations with the experimental data.

As can be seen in the upper part of Fig. 5, only a very small difference is expected for the Po cases as a function of neutron number, and within errors, this is in agreement with experiment.

However, we also obtain nearly identical results for the Pb isotones, indicating that in this formulation, the presence of the two $\pi s_{1/2}$ holes does not change the core properties sufficiently to affect the magnetic moment. As a result, there is a significant discrepancy between this theoretical approach and the experimental values for ^{194}Pb and ^{196}Pb. Contributions other than the coupling of the valence protons and the quadrupole vibrations of the underlying Hg core must be sought to explain the results for the lighter Pb isotopes.

2. *Influence of the particle-octupole vibration coupling on the magnetic moments*

The enhanced $11^-\rightarrow 8^+$ $E3$ transitions observed in the lighter Pb and Po isotopes ($N\leqslant 114$) can be associated with a single orbit change involving the proton transitions $\pi 1i_{13/2}\rightarrow 2f_{7/2}$ and $\pi 1i_{13/2}\rightarrow 1h_{9/2}$ because of octupole admixtures [24]. In the Rn isotopes, the same $\pi(2f_{7/2}\otimes 3_1^-)$ and $\pi(1h_{9/2}\otimes 3_1^-)$ admixtures (and others) need to be taken into account explicitly to explain simultaneously the enhanced $E3$ decay from, and the magnetic moments of, numerous isomeric states [34–36]. A similar approach has been applied here to investigate the influence of the octupole coupling on the magnetic moments of the 11^- isomers.

In this case, the coupling leads specifically to $\pi[1h_{9/2}(2f_{7/2}\otimes 3^-)]_{11^-}$ and $\pi[1h^2_{9/2}\otimes 3^-]_{11^-}$ admixtures. The basis used was restricted to three states: $|1h_{9/2}1i_{13/2}\rangle$, $|1h_{9/2}(2f_{7/2}\otimes 3_1^-)\rangle$, and $|1h^2_{9/2}\otimes 3_1^-)\rangle$. The diagonal terms depend on the single-particle energies (experimental energies corrected for their octupole contributions), the energies of 3^- vibration for the coupled case, and the additional particle-particle interactions available from empirical values, or the theoretical values of Kuo and Herling [37]. The off-diagonal elements are the particle-octupole vibration matrix elements deduced from the properties of the 3^- vibrations [38,39], and the off-diagonal shell-model matrix elements by Kuo and Herling [37]. The wave function $|\overline{11^-}\rangle=c|1h_{9/2}1i_{13/2}\rangle + d|1h_{9/2}(2f_{7/2}\otimes 3_1^-)\rangle + e|1h^2_{9/2}\otimes 3_1^-\rangle$ is calculated by diagonalizing the three-dimensional matrix. The g factor

$$g = c^2g(|1h_{9/2}1i_{13/2}\rangle) + d^2g[|1h_{9/2}(2f_{7/2}\otimes 3_1^-)\rangle] + e^2g[|1h^2_{9/2}\otimes 3_1^-\rangle] \quad (8)$$

is obtained by taking the single-particle g factors for the $1h_{9/2}$, $1i_{13/2}$, $2f_{7/2}$, and 3_1^- states of Ref. [36] and combining them through the Landé formula.

Since the mixing depends on the properties of the 3^- core, which is not known in the lighter isotopes, we have carried out the calculation as a function of the octupole energy, with appropriate scaling of the core $E3$ strength [40]. Figure 6 shows the dependence of the calculated g factor on the octupole energy as the energy is reduced from that known in ^{208}Pb. A slight decrease with decreasing octupole energy is obtained, but in general there is little sensitivity to the admixtures. This is mainly because the relatively large g factor from the $f_{7/2}$ proton is compensated for by the relatively

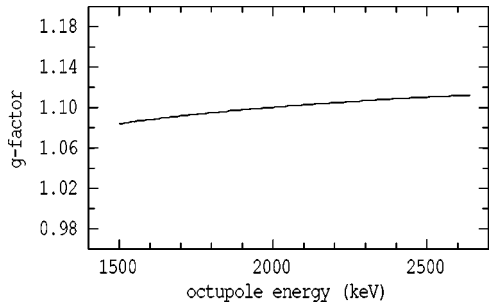

FIG. 6. g factors for the 11^- configuration from a particle-octupole vibration model as a function of the octupole energy.

small g factor of the 3^- vibration. The net result of adding a component where these are coupled together, is therefore minimal. Again, these effects would not be able to account for the observed g factor values unless the octupole energy were lowered to an extreme value.

3. Nilsson approach

The first step in considering the g factor to be expected in the case of a well-defined deformation, where the Nilsson prescription can be used, is to choose effective spin and orbital g factors, which reproduce the spherical values. The spherical values for the $h_{9/2}$ orbital and others have been evaluated in detail by Stuchbery *et al.* [41,42]. Fits to the octupole-corrected empirical values [41,42] imply that effective values, $g_l^{eff.}=1.115$ and $g_s^{eff.}=3.310$ are appropriate for the $h_{9/2}$ proton.

The Nilsson-model calculation from which the average intrinsic spin projection calculation $\langle S_z\rangle$ is deduced was carried out using the potential parameters for the $N=5$ and 6 shells chosen by Bengtsson and Ragnarsson [43] for the neutron-deficient Au region. The value of $\langle S_z\rangle$ for the $9/2^-[505]$ orbital from the $h_{9/2}$ proton is not strongly dependent on the magnitude of the deformation since it is almost pure, but there is significant admixture of the $h_{11/2}$ orbital leading to $\langle S_z\rangle=-0.344$ at $\epsilon_2=-0.18$ (approximately the predicted deformation), compared to $\langle S_z\rangle=-0.409$ at sphericity. The value of g_Ω is given by

$$g_\Omega = g_l^{eff.} - (g_l^{eff.} - g_s^{eff.}) \times \frac{\langle S_z\rangle}{\Omega}. \tag{9}$$

Substitution in Eq. (9) gives $g_{9/2}=+0.947$ for $\varepsilon_2=-0.18$.

For the $i_{13/2}$ proton, $\langle S_z\rangle=+0.500$ independent of deformation, but since there are significant octupole admixtures at sphericity, it is more appropriate to take the empirical value $g_\Omega=g=1.246(14)$ for the $13/2^+[606]$ orbital rather than the pure Nilsson value of $g=1.284$. The g_K value for a state with $K=\Omega_1+\Omega_2$ is

$$g_K = \frac{1}{K}(\Omega_1 g_{\Omega_1} + \Omega_2 g_{\Omega_2}),$$

which gives

$$g_{11} = \frac{1}{11}\left(\frac{9}{2}\times 0.947 + \frac{13}{2}\times 1.246\right) = 1.124$$

for the 11^- configuration. If the 11^- state is a bandhead, which is the case in principle, rotation must be taken into account with the formula

$$g = g_R + (g_K - g_R)\times\frac{K}{I+1} = 1.055,$$

where a value for the collective g factor of $g_R=0.30$ has been used. This value for $g(11^-)$ is indeed very close to the observed values for both ^{194}Pb and ^{196}Pb. Alternative ways of estimating the g_Ω value for the $13/2^+[606]$ orbital lead to very similar values with a small variation in the estimate of $g(11^-)$. The shaded area in the lower panel of Fig. 5 indicates the range of the prediction including the uncertainty in the $i_{13/2}$ g_Ω value and the deformation range ε_2 from -0.15 to -0.18. To the extent that this is a valid approach, then, it provides good support for the description of the 11^- isomers as being oblate deformed, with the further implication that such an oblate deformation is not present in the Po isotopes. The main difference, of course, is that the g factor is lowered because of the inclusion of a collective angular momentum component.

IV. SUMMARY AND CONCLUSIONS

We have measured the g factors of the 9^- and 11^- isomers in ^{194}Pb and ^{196}Pb, thus allowing for a systematic study of the configuration of such states in the Pb isotopes. A more extended analysis of the g factors of the 9^- states in ^{200,202}Pb than was possible previously, shows that the 9^- state has mainly the $|2f_{5/2}^{-1}1i_{13/2}^{-1}\rangle$ configuration, but that small intensities of other components must be present. For lower neutron numbers ($N=112,114$) this remains the dominant configuration with $|2f_{7/2}^{-1}1i_{13/2}^{-1}\rangle$ admixtures (proposed by some calculations) being severely limited.

The g factors of the 11^- isomers in Pb are smaller than the values in the Po isotones, which themselves have values close to the spherical limit represented by the g factor of the ^{210}Po(11^-) isomer. The effects of particle-quadrupole and particle-octupole vibration couplings are not found to be significant. Since nearly the same theoretical values are predicted in these calculations, for the magnetic moments in both Po and Pb nuclei, within the particle-vibration model at least, the presence of the $\pi 3s_{1/2}$ holes does not apparently affect the magnetic moments to the extent that it affects the quadrupole moments.

The smaller values obtained for the Pb g factors are in fact, in quantitative agreement with the presence of a moderate oblate deformation, which is expected to be better developed in Pb than in Po. This deduction is in agreement

with the conclusion of quadrupole moment measurements [25,26]. The g factor values can then be reproduced by the Nilsson model with nominal potential parameters, when renormalizations appropriate to the matching of the spherical values for the $h_{9/2}$ and $i_{13/2}$ orbitals are used.

ACKNOWLEDGMENTS

K.V. acknowledges financial support from the Flemish Science Foundation (FWO-Vlaanderen). G.J.L. is supported through the Australian Research Council Discovery Grant No. DP0345844.

[1] P. Raghavan, At. Data Nucl. Data Tables **42**, 189 (1989), and references therein.
[2] N. Stone (unpublished).
[3] C. Stenzel, H. Grawe, H. Haas, H.-E. Mahnke, and K. H. Maier, Nucl. Phys. **A411**, 248 (1983).
[4] C. Roulet, G. Albouy, G. Auger, J. M. Lagrange, M. Pautrat, K. G. Rensfelt, H. Richel, H. Sergolle, and J. Vanhorenbeeck, Nucl. Phys. **A285**, 156 (1977).
[5] L. E. Young, S. K. Bhattacherjee, R. Brenn, B. A. Brown, D. B. Fossan, and G. D. Sprouse, Phys. Rev. C **12**, 1242 (1975).
[6] C. Stenzel, H. Grawe, H. Haas, H.-E. Mahnke, and K. H. Maier, Z. Phys. A **322**, 83 (1985).
[7] J. Penninga, W. H. A. Hesselink, A. Balanda, A. Stolk, H. Verheul, J. van Klinken, H. J. Riezebos, and M. J. A. de Voight, Nucl. Phys. **A471**, 535 (1987).
[8] A. Maj, H. Grawe, H. Kluge, A. Kuhnert, K. H. Maier, R. A. Meyer, J. Recht, and N. Roy, Z. Phys. A **324**, 123 (1986).
[9] R. Lutter, O. Häusser, D. J. Donahue, R. L. Hershberger, F. Riess, H. Bohn, T. Faestermann, F. v. Feilitzsch, and K. E. G. Löbner, Nucl. Phys. **A229**, 230 (1974).
[10] M. Anselment, W. Faubel, S. Göring, A. Hanser, G. Meisel, H. Rebel, and G. Schatz, Nucl. Phys. **A451**, 471 (1986).
[11] O. Häusser, T. K. Alexander, J. R. Beene, E. D. Earle, A. B. McDonald, F. C. Khanna, and I. S. Towner, Nucl. Phys. **A273**, 253 (1976).
[12] G. Neyens, Rep. Prog. Phys. **66**, 633 (2003).
[13] E. Recknagel, in *Nuclear Spectroscopy and Reactions*, edited by J. Cerny (Academic, New York, 1974), Part C, p. 93.
[14] J. J. Van Ruyven, J. Penninga, W. H. A. Hesselinck, P. Van Nes, K. Allaart, E. J. Hengeveld, H. Verheul, M. J. A. de Voight, Z. Sujkowski, and J. Blomqvist, Nucl. Phys. **A449**, 579 (1986).
[15] B. Fant *et al.*, J. Phys. G **17**, 319 (1991).
[16] G. D. Dracoulis *et al.* (unpublished).
[17] J. M. Rocard, M. Bloom, and L. B. Robinson, Can. J. Phys. **37**, 522 (1959).
[18] F. D. Feiock and W. R. Johnson, Phys. Rev. Lett. **21**, 785 (1968).
[19] C. Pomar, J. Blomqvist, R. J. Liotta, and A. Insolia, Nucl. Phys. **A515**, 381 (1990).
[20] W. W. True, Phys. Rev. **168**, 1388 (1968).
[21] M. Pautrat, G. Albouy, J. C. David, J. M. Lagrange, N. Poffé, C. Roulet, H. Sergolle, J. Van-horenbeeck, and Abou-Leila, Nucl. Phys. **A201**, 449 (1973).
[22] R. Bengtsson and W. Nazarewicz, Z. Phys. A **334**, 269 (1989).
[23] N. A. Smirnova, P.-H. Heenen, and G. Neyens, Phys. Lett. B **569**, 151 (2003).
[24] G. D. Dracoulis, T. Kibédi, A. P. Byrne, A. M. Baxter, S. M. Mullins, and R. A. Bark, Phys. Rev. C **63**, 061302(R) (2001).
[25] K. Vyvey *et al.*, Phys. Rev. Lett. **88**, 102502 (2002).
[26] K. Vyvey, D. Borremans, N. Coulier, R. Coussement, G. Georgiev, S. Teughels, G. Neyens, H. Hübel, and D. L. Balabanski, Phys. Rev. C **65**, 024320 (2002).
[27] K. Vyvey *et al.*, Phys. Lett. B **538**, 33 (2002).
[28] K. Heyde, Hyperfine Interact. **75**, 69 (1992).
[29] A. Arima and H. Sagawa, Phys. Lett. B **173**, 351 (1986).
[30] Amos de-Shalit and Igal Talmi, *Nuclear Shell Theory* (Academic, New York/London, 1963), p. 54.
[31] S. Raman, C. W. Nestor, S. Kahane, and K. H. Bhatt, At. Data Nucl. Data Tables **42**, 1 (1989).
[32] K. L. G. Heyde, *The Nuclear Shell Model*, 2nd ed. (Springer, New York, 1994).
[33] W. R. Kölbl, J. Billowes, J. Burde, M. A. Grace, and A. Pakou, Nucl. Phys. **A448**, 123 (1986).
[34] A. R. Poletti, G. D. Dracoulis, A. P. Byrne, A. E. Stuchbery, S. J. Poletti, and J. Gerl, Phys. Lett. **154B**, 263 (1985).
[35] S. J. Poletti, G. D. Dracoulis, A. R. Poletti, A. P. Byrne, A. E. Stuchbery, and J. Gerl, Nucl. Phys. **A448**, 189 (1986).
[36] A. E. Stuchbery, G. D. Dracoulis, A. P. Byrne, S. J. Poletti, and A. R. Poletti, Nucl. Phys. **A482**, 692 (1988).
[37] T. T. S. Kuo and G. H. Herling, Naval Research Laboratory, Washington, Report No. 2258, 1971.
[38] I. Hamamoto, Phys. Rep., Phys. Lett. **10**, 63 (1974).
[39] A. Bohr and B. Mottelson, *Nuclear Structure*, Vol. II (Benjamin, New York, 1975).
[40] G. D. Dracoulis, F. Riess, A. E. Stuchbery, R. A. Bark, S. L. Gupta, A. M. Baxter, and M. Kruse, Nucl. Phys. **A493**, 145 (1989).
[41] A. E. Stuchbery, A. P. Byrne, G. D. Dracoulis, B. Fabricius, and T. Kibédi, Nucl. Phys. **A555**, 355 (1993).
[42] A. E. Stuchbery, A. P. Byrne, and G. D. Dracoulis, Nucl. Phys. **A555**, 369 (1993).
[43] T. Bengtsson and I. Ragnarsson, Nucl. Phys. **A436**, 14 (1985).